ELSEVIER

Lithos 59 (2001) 153–170

LITHOS

www.elsevier.com/locate/lithos

High-Mg potassic rocks from Taiwan: implications for the genesis of orogenic potassic lavas

Sun-Lin Chung [a,*], Kuo-Lung Wang [a], Anthony J. Crawford [b], V.S. Kamenetsky [b], Cheng-Hong Chen [a], Ching-Ying Lan [c], Chang-Hwa Chen [c]

[a] *Department of Geosciences, National Taiwan University, 245 Choushan Road, Taipei 106-17, Taiwan*
[b] *School of Earth Sciences and Center for Ore Deposit Research, University of Tasmania, Hobart, Tasmania 7001, Australia*
[c] *Institute of Earth Sciences, Academia Sinica, P.O. Box 1-55, Nankang, Taipei, Taiwan*

Received 27 October 2000; accepted 5 October 2001

Abstract

Taiwan is an active mountain belt formed by oblique collision between the Luzon arc and the Asian continent. Regardless of the ongoing collision in central and southern Taiwan, a post-collisional extension regime has developed since the Plio–Pleistocene in the northern part of this orogen, and led to generation of the Northern Taiwan Volcanic Zone. Emplaced at ~ 0.2 Ma in the southwest of the Volcanic Zone, lavas from the Tsaolingshan volcano are highly magnesian ($MgO \approx 15$ wt.%) and potassic ($K_2O \approx 5$ wt.%; $K_2O/Na_2O \approx 1.6–3.0$). Whereas these basic rocks ($SiO_2 \approx 48$ wt.%) have relatively low $Al_2O_3 \approx 12$ wt.%, total $Fe_2O_3 \approx 7.5$ wt.% and $CaO \approx 7.2$ wt.%, they are extremely enriched in large ion lithophile elements (LILE, e.g. Cs, Rb, Ba, Th and U). The Rb and Cs abundances, >1000 and 120 ppm, respectively, are among the highest known from terrestrial rocks. In addition, these rocks are enriched in light rare earth elements (LREE), depleted in high field strength elements (HFSE), and display a positive Pb spike in the primitive mantle-normalized variation diagram. Their REE distribution patterns mark with slight Eu negative anomalies ($Eu/Eu^* \approx 0.90–0.84$), and Sr and Nd isotope ratios are uniform ($^{87}Sr/^{86}Sr \approx 0.70540–0.70551$; $^{143}Nd/^{144}Nd \approx 0.51268–0.51259$). Olivine, the major phenocryst phase, shows high Fo contents (90.4 ± 1.8; 1σ deviation), which are in agreement with the whole rock Mg-values (83–80). Spinel inclusions in olivine are characterized by high $Cr/Cr+Al$ ratios (0.94–0.82) and have compositions similar to those from boninites that originate from highly refractory peridotites. Such petrochemical characteristics are comparable to the Group I ultrapotassic rocks defined by Foley et al. [Earth-Sci. Rev. 24 (1987) 81], such as orogenic lamproites from central Italy, Span and Tibet. We therefore suggest that the Tsaolingshan lavas resulted from a phlogopite-bearing harzburgitic source in the lithospheric mantle that underwent a recent metasomatism by the nearby Ryukyu subduction zone processes. The lavas exhibit unique incompatible trace element ratios, with $Rb/Cs \approx 8$, $Ba/Rb \approx 1$, $Ce/Pb \approx 2$, $Th/U \approx 1$ and $Nb/U \approx 0.8$, which are significantly lower than the continental crust values and those of most mantle-derived magmas. Nonmagmatic enrichment in the mantle source is therefore required. Based on published experimental data, two subduction-related metasomatic components, i.e., slab-released hydrous fluid and subducted sediment, are proposed, and the former is considered to be more pervasive for causing the extraordinary trace element ratios observed. Our observations lend support to the notion that dehydration from subducting slabs at convergent margins, as a continuing process through geologic time,

* Corresponding author. Tel.: +886-2-8369-1242; fax: +886-2-2363-6095.
E-mail address: sunlin@ccms.ntu.edu.tw (S.-L. Chung).

PII: S0024-4937(01)00067-6

can account for the fractionation of these elemental pairs between the Earth's crust and mantle.

Keywords: Potassic lavas; Geochemistry; Phlogopite; Fluid enrichment; Taiwan

1. Introduction

K-rich rocks have been intensively studied for the purpose of understanding not only the differences between potassic ($K_2O/Na_2O>1$) and common ($Na_2O/K_2O \geq 1$) magmas, but also those between various types of potassic lavas from different tectonic settings (e.g., Bergman, 1987; Foley et al., 1987;

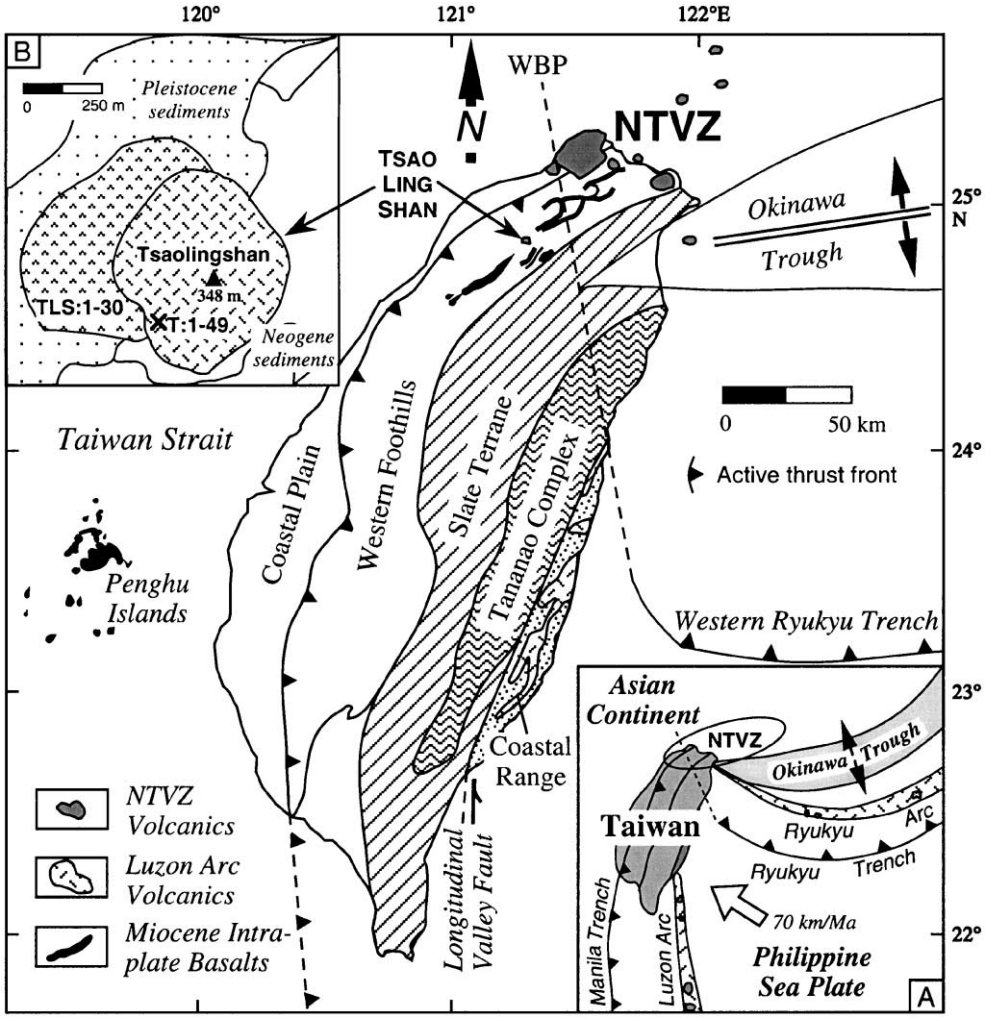

Fig. 1. The Northern Taiwan Volcanic Zone (NTVZ) and major geologic units of the Taiwan area. WBP marks the presumed western boundary of the Philippine Sea plate subduction. Inset A shows the geotectonic framework around Taiwan. Inset B shows the Tsaolingshan volcano that consists of two lava flow units. Whereas the surface samples (TLS-1 to -30) were collected from the lower unit, a cross mark on the upper unit indicates the location from which a ~50-m core was drilled for samples T-1 to -49. Compiled from Yen (1949), Chen (1990), Teng (1990), Chung et al. (1995b) and Wang et al. (1999).

Müller et al., 1992). The petrogenesis of orogenic potassic lavas, therefore, has been a subject of high interest because they are commonly emplaced in an environment with complex tectonic histories, which would facilitate better understanding and evaluating the role of various geologic processes considered responsible for the origin of enrichment in potassium (and other highly incompatible elements) of K-rich magmas. These processes include crystal fractionation, sediment subduction, crustal contamination, melt/fluid-related metasomatism and involvement of continental lithospheric mantle (e.g., Varne, 1985; Rogers et al., 1987; Foley, 1992a,b; Edwards et al., 1994; Luhr, 1997; Peccerillo, 1999; Carlson and Nowell, 2001).

In this paper, we report whole rock major and trace element and Sr–Nd isotope data, with some mineral compositions, for the Tsaolingshan rocks, which are high-Mg potassic lavas formed in the northern Taiwan mountain belt. The rocks show fine- to very fine-grained porphyritic texture and have homogeneous chemical compositions. They are furthermore characterized by trace element features including very enriched LILE and Pb, mildly enriched LREE, and relatively depleted HREE and HFSE. The overall petrological and geochemical data lead us to propose a magma origin from a refractory lithospheric mantle that experienced recent modification by the combined effect of hydrous fluid and subducted sediment derived from the neighboring Ryukyu subduction zone.

2. Geologic background

Located on the boundary between the Philippine Sea plate and the Asian plate, Taiwan is not only an active collision zone formed by the Luzon arc indentation with Asia but also a transform region between the opposing Luzon and Ryukyu subduction systems (Fig. 1). Driven by northwestward movement of the Philippine Sea plate, the northern segment of the Luzon arc is believed to have collided with the southeastern Asian continental margin since $\sim$10 Ma (Teng, 1990). The arc–continent collision, in turn, ceased continental rifting around the Taiwan Strait that began in late Cretaceous time and produced extensive intraplate basaltic volcanism during the Miocene (Chung et al., 1994, 1995a,b). Thus, the Taiwan mountain belt, composed of strata from the Asian continent in the west and the Luzon arc in the east (Fig. 1), forms and reaches a maximum altitude over 3000 m in the central region (Suppe, 1981; Teng, 1990). Although collisional tectonism is still active in most of the orogen as revealed by the prominent crustal shortening in central and southern Taiwan (e.g., Angelier et al., 1986; Tsai, 1986; Yu and Chen, 1994), structural and seismological data (Lee and Wang, 1988; Tsai, 1986; Yeh et al., 1991) demonstrate that northern Taiwan has been subjected to an episode of extensional deformation since Plio–Pleistocene time. Thus, Teng (1996) proposed that the northern part of this young mountain belt has gone through its collision orogeny and is in the process of collapsing.

3. The northern Taiwan volcanism

Northern Taiwan and its offshore islets contain a series of volcanoes, which comprise the Northern Taiwan Volcanic Zone (i.e., NTVZ; Fig. 1). Radiometric age data show that the NTVZ volcanism commenced $\sim$2.8–2.5 Ma and lasted throughout the Quaternary (Chen, 1990; Wang et al., 1999 and references therein). The NTVZ volcanic rocks consist predominantly of andesites with calc-alkaline geochemical features, and hence are conventionally regarded as products of the westward migration of the Ryukyu volcanic arc (Chen, 1990; Juang, 1993; Chung et al., 1995b; Teng, 1996). On the basis of new geochemical data, with supporting geologic and geophysical evidence, Wang et al. (1999) recently proposed that the nascent NTVZ resulted from a post-collisional extension setting owing to the Plio–Pleistocene orogenic collapse. This extensional collapse, furthermore, might have accounted for the reactivation of the opening of the Okinawa Trough that commenced in the middle Miocene (Sibuet et al., 1995) but became inactive because of the arc-continent collision in Taiwan. Consequently, the reactivated rifting in the Okinawa Trough started propagating southwestward since $\sim$1.5 Ma, with accompanying development of the westernmost part of the Ryukyu subduction system towards Taiwan (Chung et al., 2000).

Table 1
Major and trace element, and Sr–Nd isotopic data of the Tsaolingshan volcanic rocks

	TLS-3	TLS-12	TLS-17	TLS-24	TLS-27	T-20	T-24	T-30	T-43	T-48	BCR-1[a]	BHVO-1[a]	W-2[a]
Major elements (in wt.%)													
SiO_2	47.65	47.64	47.06	47.88	47.03	47.15	48.83	48.24	48.95	47.93			
TiO_2	0.80	0.82	0.82	0.81	0.80	0.92	0.82	0.83	0.83	0.79			
Al_2O_3	12.75	11.44	12.07	11.70	12.86	12.38	11.71	11.72	11.80	12.04			
Fe_2O_3[b]	7.24	7.40	7.34	7.33	7.35	8.53	7.71	7.63	7.58	7.50			
MnO	0.13	0.13	0.13	0.13	0.13	0.14	0.13	0.13	0.13	0.13			
MgO	14.72	16.07	16.01	15.16	15.32	15.52	14.21	14.24	14.25	15.50			
CaO	7.24	7.16	7.08	7.27	7.16	7.48	7.35	7.30	7.26	6.81			
Na_2O	1.91	1.74	1.72	1.83	1.77	1.83	1.89	1.92	1.84	1.73			
K_2O	4.58	5.13	5.10	5.28	5.03	2.84	5.29	5.28	5.49	5.15			
P_2O_5	1.54	1.60	1.57	1.57	1.53	1.66	1.53	1.51	1.59	1.57			
LOI	0.10	0.12	0.07	0.86	0.18	1.30	0.10	0.80	0.12	0.04			
Sum	98.66	99.25	98.97	99.82	99.07	99.75	99.57	99.60	99.84	99.19			
Mg#	81.7	82.7	82.8	82.0	82.1	80.0	80.2	80.4	80.5	82.0			
Trace elements (in ppm)													
Li	11.7	11.3	11.3	10.0	10.3	11.5	9.4	9.8	10.3	10.6	12.9	4.9 ± 0.3	9.5 ± 0.3
Be	23.8	25.0	26.3	23.7	26.0	29.0	24.9	24.5	25.9	25.9	1.6	1.06 ± 0.06	0.75 ± 0.08
Sc	25.6	25.8	25.4	28.3	27.7	29.0	29.3	28.2	28.0	27.0	32.6	31.5 ± 1.1	35.6 ± 1.4
V	140	141	141	153	189	176	143	155	152	148	407	320 ± 10	266 ± 7
Cr	965	1144	1169	992	1054	1182	1053	1056	1057	1148	16		95 ± 12
Co	41.9	44.8	44.5	44.7	47.1	49.6	44.5	44.2	43.4	47.1	37	47.0 ± 1.3	44.4 ± 1.8
Ni	437	511	512	464	484	521	457	450	437	532	13	125 ± 5	74 ± 5
Cu	33.1	29.8	33.9	31.8	34.4	38.5	27.6	34.8	32.4	32.5	19	130 ± 18	102 ± 3
Zn	43.1	43.0	45.3	47.7	58.2	52.5	48.1	52.8	48.7	52.3	129.5	116 ± 6	73 ± 3
Ga	12.0	11.8	11.9	12.0	12.8	13.9	12.8	12.7	12.8	12.7	22	22.2 ± 0.6	17.7 ± 0.5
Ge	1.3	1.3	1.3	1.3	1.3	1.5	1.4	1.3	1.3	1.3	1.5	1.64 ± 0.04	1.55 ± 0.02
Rb	2114	1045	1025	1046	1068	190	1081	1063	1266	1089	47.2	9.8 ± 0.3	20.4 ± 0.4

Sr	670	661	664	658	704	771	648	657	663	662	330	406 ± 14	197 ± 6
Y	12.9	13.1	13.1	13.1	14.6	15.6	14.4	14.3	14.0	13.9	38	29.4 ± 1.4	23.8 ± 1.2
Zr	111	111	110	109	117	125	112	115	117	114	190	177 ± 4	92 ± 3
Nb	15.4	15.3	15.2	15.0	16.2	17.1	14.6	15.4	15.7	15.5	14.0	22.3 ± 1.1	8.48 ± 0.20
Mo	0.16	0.19	0.18	0.20	0.49	0.52	0.47	0.29	0.34	0.39	1.6	1.11 ± 0.04	0.44 ± 0.04
Sn	6.9	7.3	7.0	7.4	6.7	8.7	7.2	7.3	8.9	8.0	2.7	2.6 ± 0.2	2.08 ± 0.11
Cs	174	125	122	115	124	23.6	120	113	124	118	0.96	0.103 ± 0.004	0.88 ± 0.02
Ba	997	1009	1022	885	922	979	851	864	925	920	681	142 ± 5	172 ± 2
La	26.2	25.9	26.2	23.4	23.9	26.5	24.6	24.3	24.8	24.6	24.9	15.9 ± 1.0	10.7 ± 0.3
Ce	52.0	52.2	52.9	46.7	47.7	53.1	49.0	48.2	49.0	49.1	53.7	40.6 ± 1.4	23.7 ± 0.5
Pr	6.25	6.31	6.36	5.61	5.77	6.42	5.91	5.82	5.94	5.94	6.8	5.6 ± 0.2	2.95 ± 0.07
Nd	25.6	26.0	26.3	22.9	23.2	26.3	24.1	23.8	24.5	24.3	28.8	25.6 ± 0.9	12.7 ± 0.4
Sm	4.88	4.93	5.00	4.37	4.36	4.98	4.61	4.57	4.59	4.62	6.59	6.4 ± 0.2	3.21 ± 0.07
Eu	1.14	1.22	1.21	1.07	1.06	1.25	1.09	1.15	1.13	1.11	1.95	2.10 ± 0.12	1.06 ± 0.03
Gd	3.60	3.72	3.74	3.37	3.53	3.86	3.41	3.35	3.39	3.32	6.68	6.30 ± 0.20	3.55 ± 0.12
Tb	0.51	0.52	0.53	0.47	0.46	0.54	0.50	0.49	0.48	0.48	1.05	0.96 ± 0.03	0.59 ± 0.03
Dy	2.62	2.72	2.74	2.38	2.42	2.79	2.60	2.57	2.54	2.53	6.34	5.40 ± 0.20	3.66 ± 0.13
Ho	0.53	0.55	0.55	0.48	0.48	0.57	0.53	0.52	0.52	0.51	1.26	0.97 ± 0.05	0.74 ± 0.03
Er	1.49	1.55	1.55	1.37	1.35	1.62	1.47	1.45	1.43	1.43	3.63	2.60 ± 0.10	2.13 ± 0.07
Tm	0.22	0.22	0.23	0.20	0.20	0.24	0.22	0.21	0.21	0.21	0.56	0.38 ± 0.04	0.33 ± 0.02
Yb	1.37	1.40	1.41	1.21	1.26	1.44	1.34	1.31	1.28	1.28	3.38	2.11 ± 0.09	2.00 ± 0.09
Lu	0.20	0.21	0.21	0.19	0.19	0.21	0.20	0.20	0.18	0.19	0.51	0.30 ± 0.01	0.30 ± 0.01
Hf	3.42	3.43	3.46	2.95	3.04	3.41	3.02	3.09	3.13	3.09	4.95	4.61 ± 0.21	2.34 ± 0.09
Ta	0.98	0.95	0.96	0.83	0.86	0.94	0.79	0.82	0.84	0.83	0.81	1.28 ± 0.05	0.48 ± 0.01
Pb	27.8	25.6	30.0	23.4	20.9	23.3	18.6	20.3	16.6	22.2	13.6	2.50 ± 0.40	7.80 ± 0.40
Th	22.9	22.9	23.3	19.8	18.7	21.7	19.8	19.3	20.2	19.6	5.98	1.28 ± 0.04	2.20 ± 0.05
U	21.2	21.7	22.1	18.2	17.5	20.0	17.5	17.2	17.6	18.1	1.75	0.45 ± 0.02	0.53 ± 0.02
Isotopic ratios[c]													
$^{87}Sr/^{86}Sr$	0.70546	0.70551	0.70543		0.70543	0.70542	0.70540	0.70543	0.70546	0.70551			
$^{143}Nd/^{144}Nd$	0.51268	0.51263	0.51266	0.51266	0.51266	0.51264	0.51265	0.51268	0.51266	0.51259			

Mg# = atomic 100 ($Mg/Mg + Fe^{2+}$), assuming $Fe_2O_3/FeO = 0.1$.

[a] Internal rock standards used for ICP-MS determinations (Liu et al., 1996). Calibration values of BCR-1 are from Govindaraju (1994). Analytical results of BHVO-1 and W-2 shown with 1σ errors.

[b] Total iron shown.

[c] Analytical 2σ errors are: ±0.00004 for $^{87}Sr/^{86}Sr$ and ±0.00002 for $^{143}Nd/^{144}Nd$ measurements.

Wang et al. (1999) identified a spatial geochemical change in the NTVZ. Starting from the northeast, compositions of the volcanic rocks vary from low-K through calc-alkaline to shoshonitic, and so these rocks delineate a southwestward increase in the enrichment of potassium and highly incompatible trace elements. Such a spatial variation, running subparallel with the westernmost Ryukyu Trench (Fig. 1), is distinct from that of the arc magmas whose compositional variation appears across the direction of the trenches (Gill, 1981). This unique variation observed in the NTVZ is attributed to a progressive southwestward decrease in the degree of partial melting in the mantle source region because of southwestward decrease in the lithospheric extension (Wang et al., 1999). Emplaced in the southwest of the NTVZ (Fig. 1), the Tsaolingshan lavas have been generally regarded as the youngest member originating from small degrees of melting an enriched lithospheric mantle source (cf. Chung et al., 1995b).

4. The Tsaolingshan magmas

The Tsaolingshan (Mt Tsaoling) is an isolated, cone-shaped volcano that develops on Pleistocene sediments in northwestern Taiwan. Since the pioneer work by Ichimura (1943), lavas from the Tsaolingshan volcano have been known for their K-rich nature. Based on a detailed petrographic description, along with limited major element data, these K-rich lavas has been termed absarokite by Yen (1949), a term used in following studies (Chen, 1983; Huang and Chen, 1985; Juang, 1993). The volcanic body, covering an area of ~ 1 km (inset of Fig. 1), consists mainly of lava flows with subordinate pyroclastics. Age determinations by K–Ar (Juang, 1993) and Ar–Ar (Chen, C-H., unpublished data) methods indicate that the eruption took place at ~ 0.2 Ma. Although some of the major element characteristics of the Tsaolingshan rocks, e.g. $SiO_2 \approx 48$ wt.%, $MgO \approx 15$ wt.% and $K_2O \approx 5$ wt.%, have been reported previously (Chen, 1983; Huang and Chen, 1985), high-quality trace element and isotope data were unavailable before this work.

In this study, 30 fresh samples were collected from western outcrops of the Tsaolingshan volcano (Fig. 1). After petrographic examination, 15 of the freshest were used for major element determinations. Additional 15 out of the 49 core samples that were studied by Huang and Chen (1985) were re-determined. Ten of them were analyzed for trace elements and Sr and Nd isotope ratios. All samples analyzed are porphyritic and composed of a fine- to very fine-grained groundmass. Olivine is the most abundant phenocryst phase (~ 5 vol.%). The majority of olivine is transparent and euhedral, with grain size generally being 1 mm or less. Occasionally, macrocrysts (up to 2–3 mm) of milky olivine are visible in hand specimens and show corroded texture in thin sections. Other phenocrysts include diopside, phlogopite, Fe–Ti oxide and leucite in minor amounts. The groundmass consists essentially of the same mineral assemblage, with diopside being more abundant than olivine.

5. Analytical methods

The compositions of olivine and associated spinel inclusions were analyzed using a Cameca SX50 electron microprobe at the University of Tasmania under routine operating conditions. Sample preparation and analytical procedures are the same as those reported by Kamenetsky et al. (2001). Selected rock samples were crushed, hand-picked to avoid milky olivine macrocrysts, and then powdered in a corundum mill. Major elements were determined by X-ray fluorescence techniques on fused glass beads using Rigaku® Symaltics 3550 and RIX-2000 spectrometers, respectively, at Kyoto University and National Taiwan University. The analytical procedures are the same as those described by Goto and Tatsumi (1994), yielding analytical uncertainties better than $\pm 5\%$ (2σ) for all major elements. Loss on ignition (LOI) was obtained by routine procedures. The powdered samples were dissolved using an HF/HNO_3 (10:1) mixture in screw-top Teflon beakers for 7 days at ~ 100 °C, followed by evaporation to dryness, then refluxing in 7 N HNO_3 and drying again, and finally dissolving the sample cake in 2% HNO_3. An internal standard solution of 10-ppb Rh was added and the spiked dissolutions were diluted with 2% HNO_3 to a sample/solution weight ratio of 1:1000. The internal standard was used for monitoring the signal shift during inductively coupled plasma-mass spectrometry (ICP-MS) measurements

using a Perkin Elmer® Elan-6000 spectrometer at the Guangzhou Institute of Geochemistry, China, which shows a good stability range within ~10% variation (Liu et al., 1996). Values recommended for the USGS rock standard BCR-1 (Govindaraju, 1994) were used for data calibrations; the analytical errors are generally better than ±5% (2σ) for most trace elements as shown by the statistics of duplicate analyses on two additional rock standards BHVO-1 and W-2 (Table 1). The samples were dissolved for Sr and Nd separation using routine cation-exchange column techniques. Sr and Nd isotopic ratios were determined by VG354® (Sr) and Finnigan MAT262® (Nd) mass spectrometers, respectively, at the Academia Sinica, Taipei. Further analytical details are available in Chen et al. (1990). The isotopic ratios were corrected for mass fractionation by normalizing to $^{86}Sr/^{88}Sr = 0.1194$ and $^{146}Nd/^{144}Nd = 0.7219$. Long-term laboratory measurements for NBS987 Sr and La Jolla (UCSD) Nd standards are 0.710240 ± 0.000038 (2σ) and 0.511867 ± 0.000028 (2σ), respectively.

6. Results

Representative compositions of spinel inclusions and their olivine host are given in Table 2. Whole rock elemental and isotopic data of the selected 10 samples are listed in Table 1, in which the trace element calibration values used for BCR-1 and analytical results obtained for BHVO-1 and W-2 are also presented.

6.1. Mineral composition

Olivine phenocrysts in the Tsaolingshan rocks have high-Mg compositions, with a significant range of Fo contents (94–83) and an average Fo (mol%) of 90.4 ± 1.8 (Fig. 2a). Associated with high NiO concentrations (generally ≥0.3 wt.%), their Fo values show a positive correlation with NiO and a negative correlation with CaO and MnO (Fig. 2b). The CaO contents, however, decrease as Fo ≤ 88, implying that from this composition additional liquidus phases such as diopside were involved in the crystal fractionation.

Table 2
Representative analyses of spinel inclusions and their host olivines in the Tsaolingshan volcanic rocks

Spinel	SP-1	SP-2	SP-3	SP-4	SP-5	SP-6	SP-7	SP-8	SP-9	SP-10
SiO_2	0.21	0.34	0.10	0.24	0.10	0.07	0.03	0.03	0.12	0.08
TiO_2	0.32	0.87	0.29	0.29	0.45	0.51	1.02	1.03	0.41	0.29
Al_2O_3	2.68	6.61	2.79	2.65	2.67	4.85	7.86	7.64	3.01	2.84
Fe_2O_3	6.85	16.91	7.97	8.36	8.74	8.75	13.14	13.01	6.13	6.88
FeO	18.55	20.10	18.19	15.05	19.64	16.86	16.17	18.52	11.78	14.78
MnO	0.32	0.27	0.31	0.17	0.35	0.23	0.19	0.27	0.16	0.09
MgO	9.09	8.63	8.97	11.23	8.45	10.42	11.48	9.98	13.56	11.44
Cr_2O_3	62.47	46.39	60.15	61.56	60.17	57.96	49.77	49.71	64.52	62.72
Total	100.50	100.12	98.76	99.55	100.57	99.64	99.65	100.20	99.68	99.13
$Mg/Mg+Fe^{2+}$	46.63	43.34	46.79	57.08	43.42	52.42	55.85	49.00	67.24	57.98
Cr/Cr + Al	93.98	82.49	93.54	93.98	93.80	88.92	80.94	81.35	93.50	93.68
Fe^{2+}/Fe^{3+}	3.01	1.32	2.54	2.00	2.50	2.14	1.37	1.58	2.13	2.39
Host Olivine										
SiO_2	40.82	40.68	40.80	41.57	40.55	41.29	41.32	40.37	41.59	40.98
FeO[a]	8.12	11.08	9.07	7.35	11.25	8.19	8.55	10.61	5.62	7.79
MnO	0.15	0.21	0.16	0.16	0.26	0.14	0.18	0.28	0.10	0.14
MgO	49.78	47.70	48.59	51.07	47.26	49.29	49.69	47.71	51.74	50.40
CaO	0.15	0.14	0.11	0.08	0.20	0.14	0.18	0.19	0.07	0.04
NiO	0.39	0.25	0.35	0.41	0.27	0.36	0.25	0.29	0.37	0.44
Cr_2O_3	0.13	0.07	0.14	0.15	0.11	0.03	0.15	0.07	0.04	0.13
Total	99.54	100.13	99.22	100.79	99.89	99.44	100.34	99.51	99.53	99.93
Fo (Mg#)	91.6	88.5	90.5	92.5	88.2	91.5	91.2	88.9	94.3	92.0

[a] Total iron.

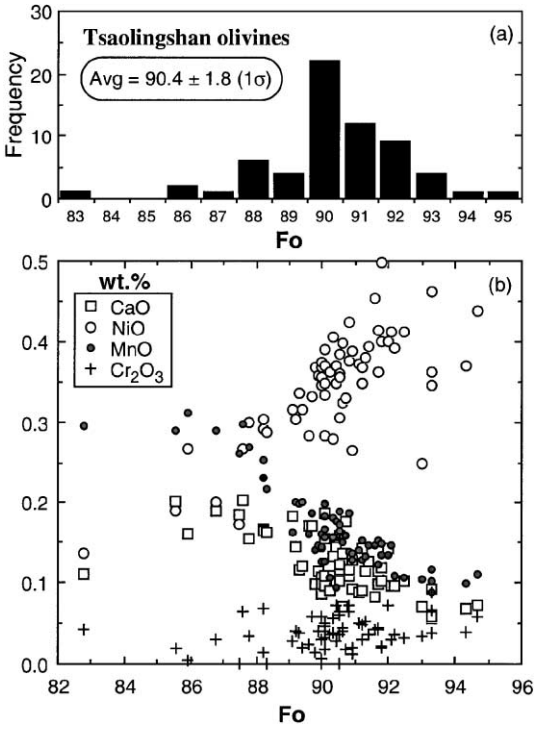

Fig. 2. Plots of olivine phenocryst compositions for the Tsaolingshan rocks, showing (a) forsterite content variation and (b) minor oxides plotted against the forsterite contents.

The Cr#, i.e., (Cr/Cr + Al), of spinels from high-Mg magmas has been widely applied to discriminate between fertile (lherzolite) and refractory (harzburgite) mantle sources (cf. Dick and Bullen, 1984; Arai, 1994). Spinels from the Tsaolingshan lavas exhibit a wide range of composition, with Cr# ≈ 94–80 and Al_2O_3 ≈ 2–8 wt.% (Table 2 and Fig. 3). The very high Cr# (up to 94) and low Al_2O_3 of the Tsaolingshan spinels, together with high Fo contents in the olivine host, point to a highly refractory mantle source whose composition could be comparable to that of boninites and/or high-Mg picritic arc magmas (Eggins, 1993; Kamenetsky et al., 1995 and references therein). At a given Al_2O_3 (Fig. 3), however, they have higher TiO_2 contents than those from boninites. Interestingly, in the whole-rock composition, the Tsaolingshan lavas also show higher TiO_2 contents than those reported for experimental refractory mantle melts (Falloon et al., 1988) (see Section 6.2). Some Tsaolingshan spinels are rich in Ti and plot toward the spinel fields defined by high-K mafic rocks from the Roman Province (Vico volcano), Italy and the Bodrum complex, Turkey (Fig. 3).

6.2. Major element data

The Tsaolingshan lavas are entirely mafic (SiO_2 ≈ 47–49 wt.%) and possess remarkably high MgO (14–16 wt.%) and K_2O (5.5–4.6 wt.%). A sample (T-20) with apparently lower K_2O (2.84 wt.%) and higher LOI (Table 1) is ascribed to secondary alteration. These lavas are distinct from other NTVZ volcanic rocks, which generally have more evolved compositions and are sodium-rich (Na_2O/K_2O>1). In Fig. 4, they plot in the field of ultrapotassic lavas, in contrast to "common" NTVZ volcanic rocks whose compositions range from low-K calc-alkaline to shoshonitic (Wang, 2000). The Tsaolingshan rocks have high Mg# values [Mg# = Mg/(Mg + Fe); see footnote in Table 1] ranging from 83 to 80, indicating that they potentially represent primary melts of the mantle peridotite. These rocks exhibit low Al_2O_3 (11–13 wt.%), total

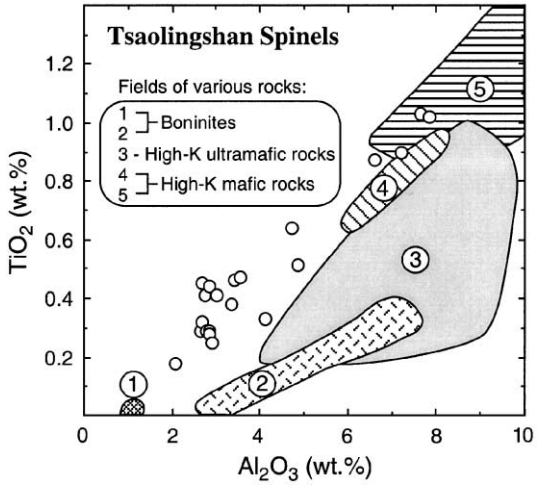

Fig. 3. TiO_2 vs. Al_2O_3 plots of spinel inclusions trapped in olivine phenocrysts (Fo = 94–87) from the Tsaolingshan rocks. Fields for comparison are low-Ti, low-Al spinel inclusions in primitive olivines from various volcanic complexes. These include: (1) low-Ca boninites from Victoria, Australia (Crawford, 1980); (2) low-Ca boninites from Cape Vogel, PNG (Walker and Cameron, 1983) and high-Ca boninites from the Hunter Ridge–Hunter Fracture Zone (Sigurdsson et al., 1993); (3) high-K ultramafic lavas from Vanuatu (Eggins, 1993) and East Kamchatka (Kamenetsky et al., 1995); (4) high-K basalts from Vico, Italy (Barbieri et al., 1988); and (5) high-K mafic rocks from Bodrum, Turkey (Robert et al., 1992).

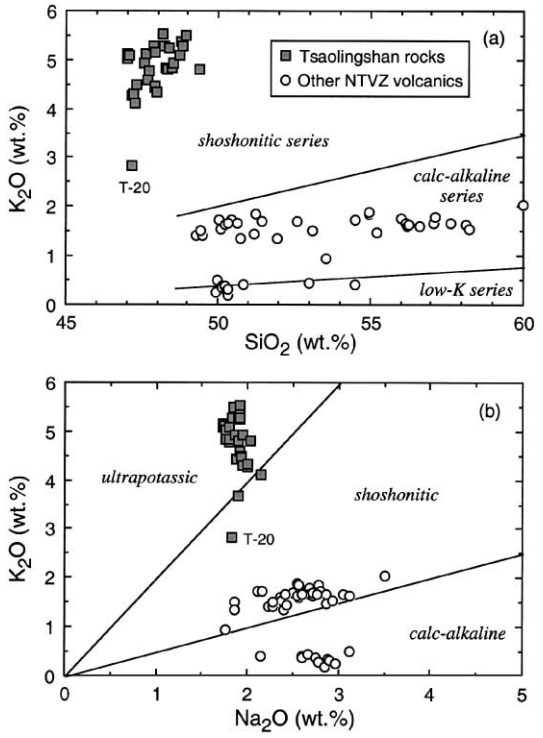

Fig. 4. Plots of K_2O vs. (a) SiO_2 and (b) Na_2O for the Tsaolingshan rocks, showing their K-rich nature relative to other NTVZ volcanics. The rock series boundaries in (a) and (b) are from Gill (1981) and Peccerillo and Taylor (1976), respectively.

Fe_2O_3 (7.2–8.5 wt.%) and CaO (6.8–7.5 wt.%). In a TiO_2 vs. total Fe_2O_3 plot (Fig. 5), they are comparable to the lamproitic rocks from Italy, Spain and Tibet that all plot close to the field defined by experimental melts of depleted peridotite (Falloon et al., 1988). In analogy with these lamproites, the Tsaolingshan lavas can be explained as small degree melts derived from a refractory mantle source; and the relatively higher TiO_2 contents may reflect small degrees of melting that could produce lavas with raised TiO_2 than the large degree melts (Schaefer et al., 2000). In terms of CaO and Al_2O_3 contents, the Tsaolingshan lavas are similar to the Italian lamproites, which have been proposed as originating from a harzburgitic mantle source contaminated by sediment subduction (cf. Peccerillo, 1999). Excluding the altered sample (T-20), the rocks we analyzed show a fairly uniform major element composition.

6.3. Trace element data

The whole-rock compositional uniformity is also observed in trace elements. The 10 Tsaolingshan samples have similar REE concentration levels (Table 1). In the REE variation diagram (Fig. 6a), they delineate a uniform pattern showing enriched LREE ($La_N \approx 100$; normalized to the chondritic values from Sun and McDonough, 1989). The rocks display slight Eu negative anomalies ($Eu/Eu^* \approx 0.90-0.84$), and are relatively depleted in HREE ($Lu_N \approx 8$) than other NTVZ calc-alkaline volcanic rocks. The trace element homogeneity is also revealed in the primitive mantle-normalized variation diagram (Fig. 6b). The only "exception" is the altered sample T-20, which has much lower Cs and Rb although the alteration effect on other elements seems to be insignificant (Table 1). This sample will be excluded in the plots and discussion regarding alkali elements. The Tsaolingshan lavas are very enriched in LILE (e.g. Cs, Rb, Ba, Th and U) and Pb, mildly enriched in P and LREE, and depleted in HFSE (Nb, Ta and Ti) and HREE (Fig. 6b). Thus, the LILE/REE ratios are typically high. Their overall major and trace element characteristics are generally comparable to those of orogenic lamproites from the Betic Cordillera, SE Spain (Turner et al., 1999), central Italy (Peccerillo, 1999) and the Tibetan plateau (Chung et al., 1998; Miller et al., 1999), which belong to the Group I ultrapotassic rocks classified by Foley et al. (1987). The Tsaolingshan lavas are particularly enriched in Cs and Rb, with Cs

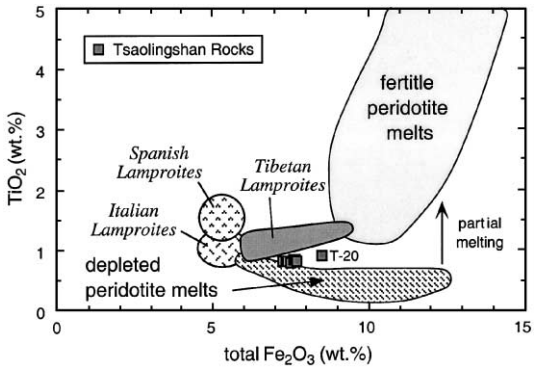

Fig. 5. Plots of TiO_2 vs. total Fe_2O_3 for the Tsaolingshan rocks compared with fields for some orogenic lamproites (Miller et al., 1999; Peccerillo, 1999; Turner et al., 1999) and experimental peridotite melts (Falloon et al., 1988).

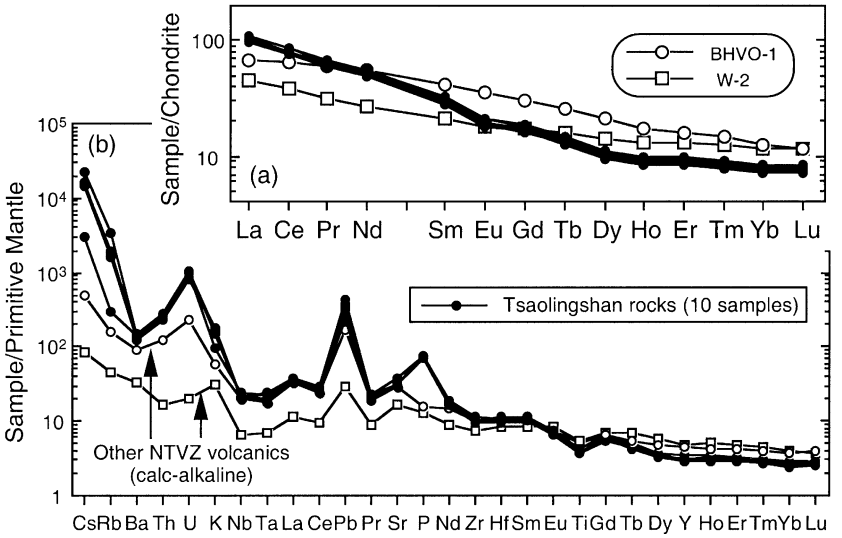

Fig. 6. (a) Chondrite-normalized REE variation diagram for the Tsaolingshan rocks which all mark with small but apparent negative Eu anomalies, with Eu/Eu* (the observed value divided by that extrapolated from the Sm and Gd concentrations) = 0.90 – 0.84. REE patterns obtained for the two internal rock standards, BHVO-1 and W-2, are also drawn. (b) Primitive mantle-normalized variation diagram for the Tsaolingshan rocks. Two calc-alkaline NTVZ samples (Wang et al., 1999) are plotted for comparison. Chondrite and primitive mantle normalizing values are from Sun and McDonough (1989).

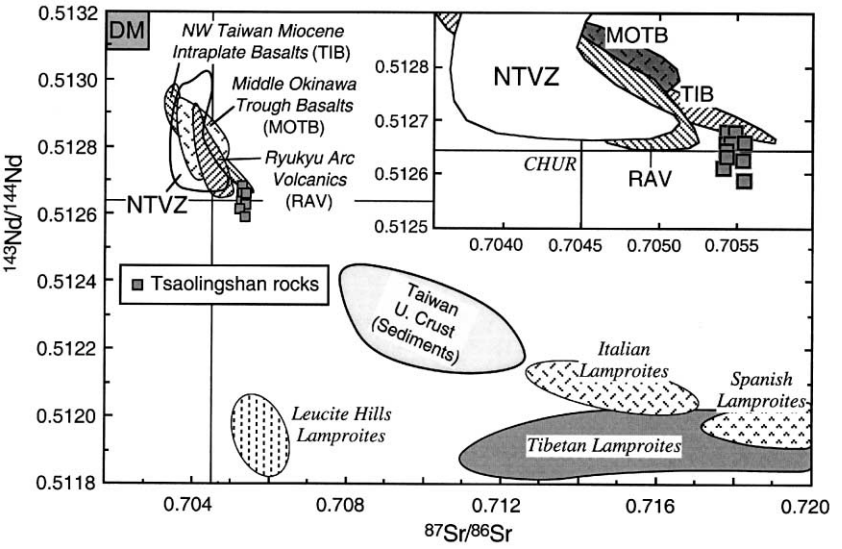

Fig. 7. The $^{87}Sr/^{86}Sr$ vs. $^{143}Nd/^{144}Nd$ diagram for the Tsaolingshan rocks compared with other NTVZ rocks (Wang, 2000), Miocene basalts from NW Taiwan (Chung et al., 1995a), Middle Okinawa Trough basalts and Ryukyu arc volcanics (Shinjo et al., 1999). Fields for Taiwan upper crust and sediments (Lan et al., 1990) and orogenic lamproites from Italy, Spain, Tibet and Leucite Hills (Peccerillo, 1999; Turner et al., 1999; Miller et al., 1999) are also shown. An enlarged view for the Taiwanese rocks is given in the inset. DM = depleted mantle; CHUR = chondritic uniform reservoir.

up to 170 ppm and Rb over 1000 ppm (Table 1), which are apparently higher than those of K-rich magmas worldwide (cf. Bergman, 1987; Müller et al., 1992) and among the highest values ever reported for terrestrial rocks.

6.4. Radiogenic isotope ratios

The 10 samples are characterized by uniform Sr and Nd isotope ratios, with $^{87}Sr/^{86}Sr \approx 0.70540-0.70551$ and $^{143}Nd/^{144}Nd \approx 0.51268-0.51259$ (Table 1), which plot around the lower right side of the isotope ranges for the NTVZ and Ryukyu arc lavas (Fig. 7). It is noted that the Sr and Nd isotope ratios of the altered sample T-20 remain unchanged and identical to other samples. The Tsaolingshan lavas plot closer to the Miocene intraplate basalts from NW Taiwan and back-arc basin basalts from the middle Okinawa Trough, both with a dominant asthenospheric mantle source (Chung et al., 1994; Shinjo et al., 1999), but away from the field for Taiwan upper continental crust and sediments. Compared to the orogenic lamproites from Italy, Spain and Tibet, they show significantly lower Sr and higher Nd isotope ratios (Fig. 7). So far, no systematic Pb isotope analysis has been carried out after the work by Sun (1980), which reported $^{206}Pb/^{204}Pb = 18.47$, $^{207}Pb/^{204}Pb = 15.64$, and $^{208}Pb/^{204}Pb = 38.79$ for a Tsaolingshan sample. The data were interpreted as indicating a magma source region that had been modified by sediments via the Ryukyu subduction zone processes (Sun, 1980). Because of the chemical and isotopic uniformity in the whole Tsaolingshan lava suite, this only set of Pb isotope data is considered to be informative and representative.

7. Discussion

7.1. Mantle source and genesis of the Tsaolingshan lavas

The high Cr# (and low Al) nature of the Tsaolingshan spinels, along with high Fo contents of the olivine host, as noted above, suggest a refractory magma source similar to that of boninites or other high-Mg arc magmas. This is consistent with the whole-rock compositional data, which show high Mg-values (and corresponding Ni and Cr) associated with low Al_2O_3, total Fe_2O_3 and CaO contents denoting a restitic peridotite mantle source that underwent previous extraction of basaltic melts. Thus, similar to the Italian lamproites (Peccerillo, 1999), the Tsaolingshan lavas represent primary or near-primary melts derived from a harzburgitic source. Such a refractory source domain, residing most likely in the continental lithospheric mantle, must have been metasomatized by enrichment events before being melted to produce the lavas that are potassic and highly enriched in incompatible trace elements such as LILE and LREE. A key question remaining is when and how the enrichment could have taken place underneath northern Taiwan.

Before exploring the mantle enrichment, it is worthwhile to discuss the vein-plus-wall-rock melting model proposed by Foley (1992b) for the genesis of potassic magmas. Whereas there is little doubt that peridotite is the volumetrically dominant constituent of the mantle, the contribution of olivine-poor lithologies (i.e., pyroxenite, eclogite and/or phlogopite/amphibole-rich veins) to various types of mantle-derived melts in different tectonic settings has become a growing subject of investigation. Recent Re–Os isotope studies for potassic lavas (e.g., Schaefer et al., 2000; Carlson and Nowell, 2001) provide convincing evidence for melting of pyroxene- and mica-rich veins in the continental lithospheric mantle, thus in support of the vein-wall rock melting model. In the Tsaolingshan rocks, olivine phenocrysts and spinel inclusions both show rather wide compositional variations, implying that there were different melt fractions derived either from various degrees of melting or a veined peridotite in the mantle. In this sense, the uniform whole-rock composition represents simply the well-mixed or "averaged" melt composition in the magma chamber before eruption. However, the lack of low-Mg member in the Tsaolingshan lava suite does not favor a major contribution by olivine-poor (e.g., mica-rich peroxenite) veins in the magma genesis. The coupling of the above-noted major element "depletion" with the highly incompatible trace element enrichment in the Tsaolingshan rocks, moreover, misfits the expectations of vein melt-wall rock interaction scenario outlined by Foley (1992b), which would produce potassic magmas with a compositional spectrum, between a vein "end-member" showing lower Mg-values and highly enriched incompatible

elements and a wall-rock (peridotite) component of high-Mg and less enriched incompatible elements (Foley, 1992b).

Prior to the arc–continent collision, the region around Taiwan was situated in a passive continental margin marked by lithospheric extension since the late Mesozoic. Thus, extension-induced basaltic volcanism occurred in the region until ~9 Ma in late Miocene time (Chen, 1990; Chung et al., 1995b). The Miocene basalts that tap both asthenospheric and lithospheric mantle sources (Chung et al., 1994, 1995a) exhibit intraplate geochemical characteristics and contain ultramafic xenoliths in localities. The xenoliths, derived mainly from ~30–50-km depth within the lithospheric mantle, consist predominantly of harzburgitic lithologies (Yang et al., 1987). By contrast, the NTVZ volcanic rocks that postdate the collision are dominated by calc-alkaline lavas and show apparent HFSE depletions (Chen, 1990; Wang et al., 1999; Wang, 2000). This change of the magma chemistry implies that, during the buildup of the northern Taiwan mountain belt (from late Miocene to late Pliocene time), the upper mantle domains underwent a contemporaneous enrichment related to the Ryukyu subduction zone processes (cf. Wang et al., 1999).

Radiogenic isotope data have been proven to be useful in providing not only information about the potential magma sources but also time constraints on relevant geologic events. Available Sr, Nd and Pb isotope data of the Tsaolingshan rocks can be explained by recent involvement of a sedimentary component related to the nearby Ryukyu subduction. This explanation is consistent with several lines of trace element evidence, such as the Eu anomalies (Fig. 6a) and HFSE depletions (Fig. 6b). However, certain incompatible element ratios observed in the Tsaolingshan rocks can hardly be reconciled with a simple sediment contamination. These include: $Nb/U \approx 0.8$, $Ce/Pb \approx 2$ and $Rb/Cs \approx 8$ (Fig. 8), as well as Th/U and Ba/Rb (both ~1; see Table 1). All such ratios are significantly lower than estimates for the continental crust (e.g., Taylor and McLennan, 1985; Rudnick and Fountain, 1995) and the "mantle values" (Hofmann, 1988; Sun and McDonough, 1989; McDonough and Sun, 1995). Given the general awareness that igneous processes in the mantle have a minimal effect on fractionating these elemental ratios, another type of

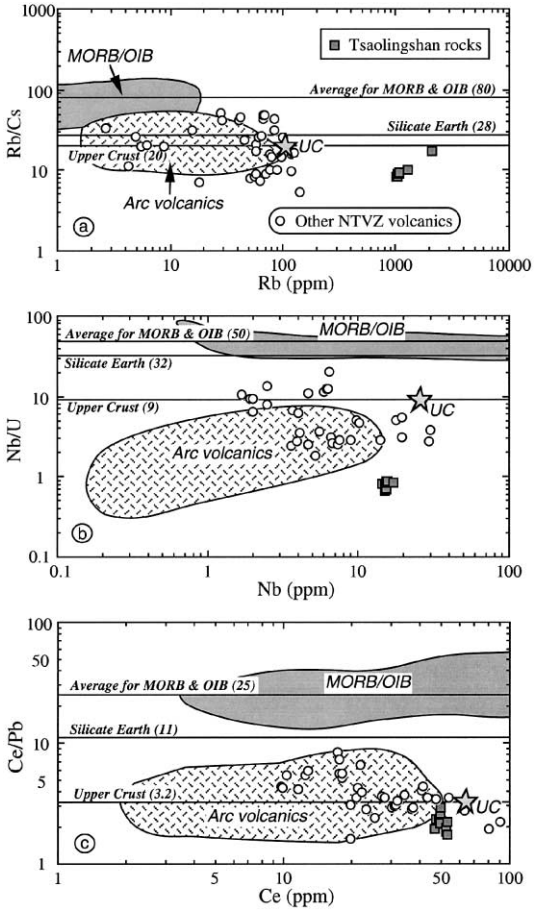

Fig. 8. Plots of (a) Rb/Cs vs. Rb, (b) Nb/U vs. Nb, and (c) Ce/Pb vs. Ce for the Tsaolingshan rocks. Data of other NTVZ volcanics are also plotted (Wang et al., 1999; Wang, 2000). Ratios for the MORB/OIB, bulk silicate Earth and upper continental crust are from Hofmann et al. (1986), McDonough et al. (1992), McDonough and Sun (1995) and Rudnick and Fountain (1995). Fields for the MORB/OIB and arc volcanics are compiled from Hofmann et al. (1986), Hart and Reid (1991), McDonough et al. (1992), Edwards et al. (1994), Miller et al. (1994), Kersting and Arculus (1995) and Pearce et al. (1995). Stars marking UC indicate the estimated upper continental crust values from Taylor and McLennan (1985) and Rudnick and Fountain (1995).

nonmagmatic enrichment is required. On the basis of mineral–aqueous fluid experiments (Brenan et al., 1995a,b; Keppler, 1996; Tatsumi and Kogiso, 1997; Ayers, 1998), we suggest such an enrichment agent to be a hydrous fluid phase derived from the neighboring Ryukyu subducting slab. In this regard, plots of Ba/La vs. $^{87}Sr/^{86}Sr$ (Fig. 9a) and Pb/Nd vs. $^{143}Nd/^{144}Nd$

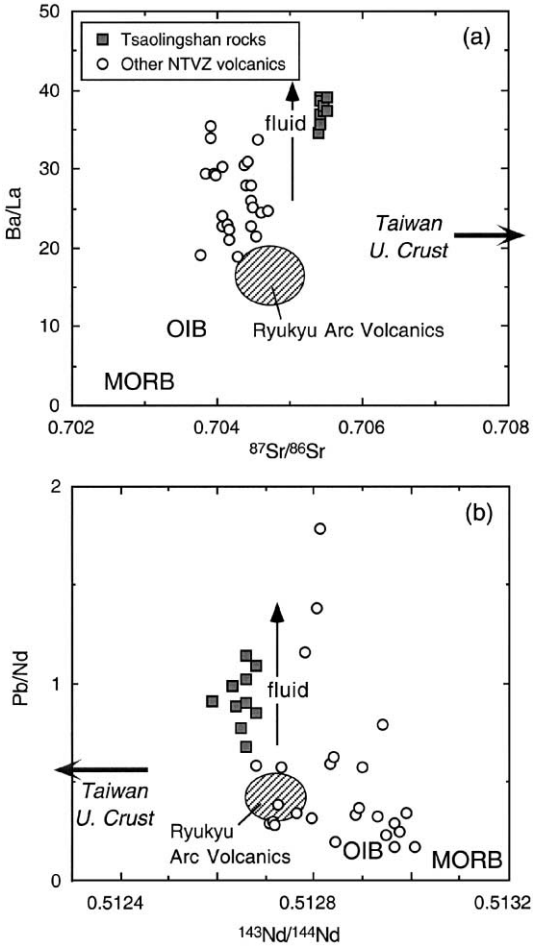

Fig. 9. Plots of (a) Ba/La vs. $^{87}Sr/^{86}Sr$ and (b) Pb/Nd vs. $^{143}Nd/^{144}Nd$ for the Tsaolingshan and NTVZ rocks. Fields for the neighboring Ryukyu arc volcanics are shown for comparison. Arrows for the fluid component and Taiwan upper crust are according to Tatsumi et al. (1986) and Lan et al. (1990), respectively. Data for OIB and MORB are from Sun and McDonough (1989).

(Fig. 9b) are presented to distinguish the magma source characteristics. The Tsaolingshan and some NTVZ rocks trend toward the fluid component and away from Taiwan upper crust. In addition, Nb/U and Ce/Pb plotted against $^{87}Sr/^{86}Sr$ (Fig. 10) are indicative of a fluid-dominating metasomatism, coupled with 10–20% contribution by the average Taiwan sediment, in the mantle source region.

To sum up, we propose that the Tsaolingshan high-Mg potassic lavas originate from a phlogopite-bearing harzburgite in the lithospheric mantle whose hybridization was ascribed to a recent metasomatism by the Ryukyu subduction zone processes. With a greatly reduced solidus temperature, such a hydrous mantle source could have been preferentially melted as a response of the geothermal perturbation caused by the post-collisional lithospheric extension in the northern Taiwan mountain belt (Wang et al., 1999). In analogy with the orogenic lamproites from Italy, Spain and Tibet, which have similar geochemical and source characteristics, we speculate the Tsaolingshan lavas to be small-degree melts. However, the melting degree must have been "large enough" to totally consume phlogopite, a major repository phase for Cs, Rb and Ba along with potassium (Schmidt et al., 1999). Residual phlogopite in the mantle source would have held back significant amounts of these elements so

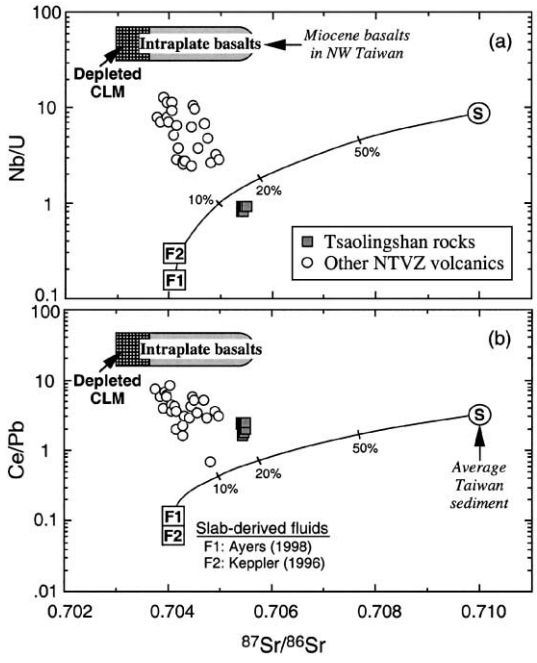

Fig. 10. Plots of (a) Nb/U and (b) Ce/Pb vs. $^{87}Sr/^{86}Sr$ ratios for the Tsaolingshan rocks. Data sources include: Chung et al. (1994, 1995a) for the Miocene intraplate basalts from NW Taiwan, Lan et al. (1990) for Taiwan sediments, and Wang (2000) for the NTVZ rocks. Small ticks marked on the mixing curve between the slab-derived fluid (F1; from Ayers, 1998) and average Taiwan sediment indicate percentages of the latter involved in the mixing calculation. In comparison with the Tsaolingshan rocks, which plot rather close to the mixing curve, most NTVZ rocks plot between the mixing curve and a depleted lithospheric mantle source.

that the lavas formed are unlikely to show the extraordinary enrichment.

7.2. Implications for the alkali enrichment in orogenic potassic lavas

As shown in Fig. 11, despite large variations in Rb/Sr and Ba/Sr, the Rb/Ba ratios of most basalts and lamproites from intraplate settings are generally similar (0.03–0.1) and close to the bulk silicate Earth estimate of ~0.09 (or Ba/Rb of ~11; McDonough et al., 1992). This observation led Rogers et al. (1987) to conclude that magmatic processes (e.g., partial melting and crystallization) have little effect on the Rb/Ba fractionation, and invoked sediment subduction for the genesis of orogenic potassic lavas that typically have high Rb/Sr and Rb/Ba ratios (Fig. 11). Subducted sediment, with composition similar to the upper continental crust, can significantly enrich Rb over both Sr and Ba in the mantle. Source contamination by sediment via subduction has been therefore widely considered responsible for the Tertiary K-rich magmatism along the Tethyan orogenic belt, as well-documented for the generation of Quaternary potassic lavas in central–south Italy (cf. Peccerillo, 1999).

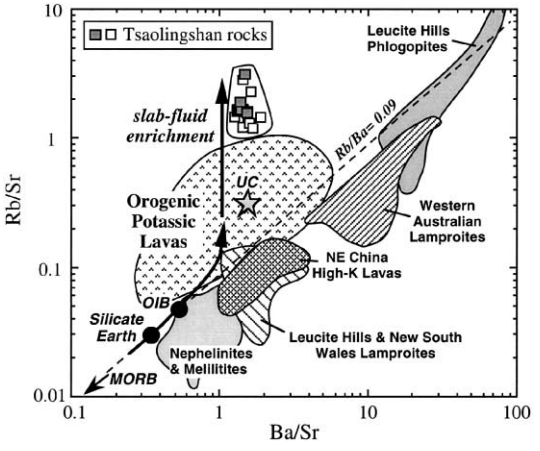

Fig. 11. Plots of Rb/Sr vs. Ba/Sr for the Tsaolingshan rocks and other potassic lavas. For the Tsaolingshan samples, solid squares are from this study and open squares are literature XRF-AA data (Chen, 1983; Huang and Chen, 1985). Data sources for the range of orogenic potassic lavas include Rogers et al. (1987), Edwards et al. (1994), Chung et al. (1998), Miller et al. (1999), Peccerillo (1999) and Turner et al. (1999). According to Peccerillo (1999), some, but not all, Italian lamproites have high Rb/Sr ratios of ~2, similar to the Tsaolingshan samples. Field for the NE China high-K lavas are based on Zhang et al. (1995). Other K-rich rock fields are after Rogers et al. (1987). Star marks the average for the upper continental crust (Taylor and McLennan, 1985). Values for OIB, MORB and the Silicate Earth are from Sun and McDonough (1989) and McDonough and Sun (1995). Note that our preferred interpretation for the extraordinarily high Rb/Sr (and Rb/Ba) ratios observed in the Tsaolingshan lavas is owing to a slab-derived fluid enrichment in the mantle source region.

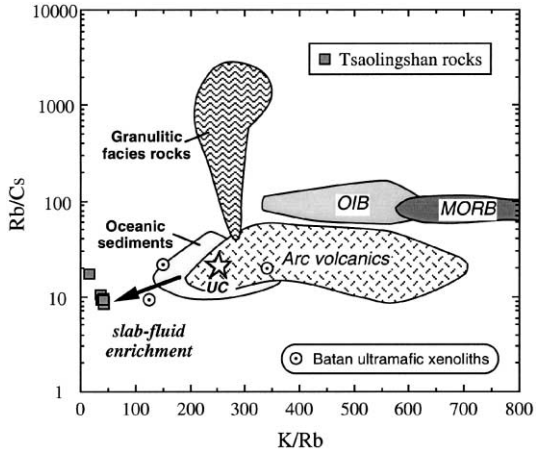

Fig. 12. Plots of Rb/Cs vs. K/Rb showing the distinction of Tsaolingshan lavas from other rocks. Comparison fields are adapted from Hart and Reid (1991). The upper continental crust value is from Rudnick and Fountain (1995) and data for the Batan ultramafic xenoliths, the Luzon arc (Philippines), are from Maury et al. (1992).

However, the alkali element enrichment in the Tsaolingshan rocks could not be interpreted simply by a sediment subduction. Together with the very high Rb and Cs, these rocks exhibit Ba/Rb ($\leq$1; Fig. 11) and Rb/Cs (~8) ratios (Fig. 8a) that are much lower than averages for the continental crust (Rudnick and Fountain, 1995) and the mantle values (McDonough et al., 1992). To explain the ubiquitous Cs enrichment relative to K and Rb in arc volcanic rocks (Fig. 12), Hart and Reid (1991) proposed a model that links granulite metamorphism with sediment subduction. These authors, adopting that granulite facies metamorphic processes would cause a large degree of Cs loss without major K and Rb depletions, advocated a Cs-enriched component from the subducted sediment under such high-grade metamorphic conditions. Experimental data reported by You et al. (1996), however, seem at odds with this scenario because LILE in

the subducted sediments would be substantially removed at much shallower depths.

In the K–Rb–Cs plots (Fig. 12), the Tsaolingshan lavas display alkali element systematics that mark with extremely low Rb/Cs and K/Rb ratios and thus are distinct from granulitic and other terrestrial rocks. An enrichment order of Cs>Rb>K, as best illustrated in the mantle-normalized variation diagram (Fig. 6b), is observed. Similar alkali enrichment has been observed in phlogopite-bearing harzburgite xenoliths from Batan, the Luzon arc (Maury et al., 1992). Three sets of whole-rock data of the Batan xenoliths are plotted between the Tsaolingshan lavas and common arc volcanics (Fig. 12). Experimental data reported by Tatsumi et al. (1986) indicate that the mobility of incompatible elements via dehydration of the subducting slab increases essentially with the ionic radius. Thus, in the slab-released hydrous fluid, the enrichment factors would be the greatest for the LILE and the alkali metals would reveal a preferential enrichment order of Cs>Rb>K. This notion is consistent with our conclusion that, although the subducted sediment is important, a hydrous fluid com-ponent should have played an even more effective role in the mantle source enrichment and hybridization that later accounted for the Tsaolingshan high-Mg potassic magmatism.

7.3. Trace element fractionation by subduction zone processes

Sharing similar bulk solid/melt partition coefficients (Hofman, 1988; Sun and McDonough, 1989), Nb and U would not be significantly fractionated during mantle melting processes, and melt compositions can reflect approximate Nb/U ratios of the mantle sources. For the Tsaolingshan rocks, their prodigious U enrichment over the neighboring Nb and Th in the mantle-normalized variation diagram (Fig. 6b), $Nb/U \approx 0.8$ and $Th/U \approx 1$, as described above, is mainly a result of source enrichment by slab-derived fluids. Significantly lower Nb/U ratios are observed in arc volcanics (Fig. 8b), different from oceanic basalts that show a nearly constant Nb/U of ~ 50 (Hofmann et al., 1986), estimated values for the bulk silicate Earth ($Nb/U \approx 32$; McDonough and Sun, 1995) and continental upper crust ($Nb/U \approx 9$; Rudnick and Fountain, 1995). Such a low Nb/U ratio range is close to that calculated for subduction-zone fluids ($Nb/U \approx 0.15-0.3$; Keppler, 1996; Ayers, 1998). This has been generally ascribed to the strong capacity of LILE and the inability to transfer significant amounts of HFSE in the slab-derived hydrous fluid. The HFSE are more likely to be stored in phases such as rutile and/or ilmenite, which may persist in the subducted slab (Ryerson and Watson, 1987). On the other hand, studies of U–Th-series isotopes (Gill and Williams, 1990; Elliott et al., 1997) and mineral–aqueous fluid partitioning experiments (Brenan et al., 1995b; Keppler, 1996; Ayers, 1998) both show that U is preferentially transported, relative to Th, from the subducting slab to the mantle wedge. Thus, significant fractionation in Th/U could occur during the dehydration process at convergent margins.

The Tsaolingshan lavas show remarkable enrichment in Pb. Their Ce/Pb ratio (~ 2; Fig. 8c) is much lower than that of average oceanic basalts ($Ce/Pb \approx 25$) and the bulk silicate Earth ($Ce/Pb \approx 11$), and slightly lower than the continental upper crust value ($Ce/Pb \approx 3.2$). However, it approximates to that of the Aleutian arc rocks (Miller et al., 1994), for which a slab-derived, low-Ce/Pb fluid phase that metasomatizes the mantle wedge has been inferred. This reduced Ce/Pb ratio is most likely caused by preferential extraction of Pb from dehydration of the subducting slab, as experimental data (Brenan et al., 1995a,b; Keppler, 1996; Ayers, 1998) suggest that Ce/Pb ratios of the slab-derived fluid would be as low as ~ 0.1 or even lower. In the fluid-modified mantle region, enrichment factors for Pb are hence greater than for K and Ba and similar to for Rb (Tatsumi et al., 1986). Hofmann et al. (1986) argued that in the Earth evolution both Nb/U and Ce/Pb ratios were fractionated by the formation of continental crust and, subsequent to this process, there was homogenization of the depleted residual mantle leading to the generation of the MORB and OIB reservoirs. A similar evolution for the Rb/Cs system has been also suggested by McDonough et al. (1992). In this case, the constant ratios of Rb/Cs, Nb/U and Ce/Pb in the MORBs and OIBs (Fig. 8) reflect simply the record in the residual mantle complementary to the continental crust extraction. This model, as pointed out by Miller et al. (1994), however, ignores the role of subduction zone processes that

can greatly fractionate these elemental pairs through dehydration.

8. Concluding remarks

The overall petrological and geochemical characteristics of the Tsaolingshan lavas allow us to conclude that the lavas were derived from a refractory lithospheric mantle source that bears phlogopite as a result of a recent metasomatism. Two types of metasomatic components, i.e., slab-released hydrous fluid and subducted sediment, both resulting from the nearby Ryukyu subduction, are suggested. The fluid-related metasomatism was more pervasive and eventually led the mantle to be hybridized and highly enriched in incompatible trace elements with extraordinary elemental ratios. This mantle source melted after the region became involved in an extensional setting owing to the Plio–Pleistocene orogenic collapse of the northern Taiwan mountain belt. The Tsaolingshan magmas, therefore, may serve as one of the most informative examples for studying not only the genesis of orogenic potassic lavas but also the elemental transfer in dehydration at convergent margins. In agreement with published mineral–fluid experimental data, the metasomatized mantle source we identify for the Tsaolingshan lavas has highly fractionated ratios of Rb/Cs, Nb/U and Ce/Pb (and Rb/Ba and Th/U as well). This observation hence reinforces the view that dehydration associated with slab subduction at convergent margins, if acting through time, could have served as the key process responsible for the fractionation of all these element pairs between the Earth's crust and mantle.

Acknowledgements

We thank C.Y. Lee and Y. Tatsumi for help with XRF analyses, X.H. Li for help with ICP-MS analyses, S. Meffre for help with electron microprobe analyses, and Shen-su Sun and Frank Yang for thoughtful discussions. Constructive journal reviews by A. Peccerillo and an anonymous reviewer significantly improved the manuscript, but the authors are responsible for any errors and omissions. This study has benefited from research grants supported by the National Science Council, Taiwan, ROC.

References

Angelier, J., Barrier, E., Chu, H.T., 1986. Plate collision and paleostress trajectories in a fold-thrust belt: the foothills of Taiwan. Tectonophysics 125, 161–178.

Arai, S., 1994. Compositional variation of olivine–chromian spinel in Mg-rich magmas as a guide to their residual spinel peridotites. J. Volcanol. Geotherm. Res. 59, 279–293.

Ayers, J., 1998. Trace element modeling of aqueous fluid–peridotite interaction in the mantle wedge of subduction zones. Contrib. Mineral. Petrol. 132, 390–404.

Barbieri, M., Peccerillo, A., Poli, G., Tolomeo, L., 1988. Major, trace element and Sr isotopic composition of lavas from Vico volcano (Central Italy) and their evolution in an open system. Contrib. Mineral. Petrol. 99, 485–497.

Bergman, S.C., 1987. Lamproites and other potassic igneous rocks: a review of their occurrence, mineralogy and geochemistry. In: Fitton, J.G., Upton, B.G.J. (Eds.), Alkaline Igneous Rocks. Geol. Soc. Spec. Publ., vol. 30, pp. 103–190.

Brenan, J.M., Shaw, H.F., Ryerson, F.J., 1995a. Experimental evidence for the origin of lead enrichment in convergent-margin magmas. Nature 378, 54–56.

Brenan, J.M., Shaw, H.F., Ryerson, F.J., Phinney, D.L., 1995b. Mineral–aqueous fluid partitioning of trace elements at 900 °C and 2.0 GPa: constraints on the trace element chemistry of mantle and deep crustal fluids. Geochim. Cosmochim. Acta 59, 3331–3350.

Carlson, R.W., Nowell, G.M., 2001. Olivine-poor sources for mantle-derived magmas: Os and Hf isotopic evidence from potassic magmas of the Colorado plateau. G^3 (Electr. J. Earth Sci.) 2, June 13.

Chen, C.-H., 1983. The geochemical evolution of Pleistocene absarokite, shoshonite and high-alumina basalt in northern Taiwan. Mem. Geol. Soc. China 5, 85–96.

Chen, C-H., 1990. The igneous rocks of Taiwan. Cent. Geol. Surv. Publ. 1, Taipei, 137 pp. (in Chinese).

Chen, C.H., Shieh, Y.N., Lee, T., Chen, C.-H., Mertzman, S.A., 1990. Nd–Sr–O isotopic evidence for source contamination and an unusual mantle component under Luzon Arc. Geochim. Cosmochim. Acta 54, 2473–2483.

Chung, S.L., Sun, S.-S., Tu, K., Chen, C.-H., Lee, C.Y., 1994. Late Cenozoic basaltic volcanism around the Taiwan Strait, SE China: product of lithosphere–asthenosphere interaction during continental extension. Chem. Geol. 112, 1–20.

Chung, S.L., Jahn, B.M., Chen, S.J., Lee, T., Chen, C.-H., 1995a. Miocene basalts in NW Taiwan: evidence for EM-type mantle sources in the continental lithosphere. Geochim. Cosmochim. Acta 59, 549–555.

Chung, S.L., Yang, T.F., Lee, C.Y., Chen, C.-H., 1995b. Igneous provinciality in Taiwan: consequence of continental rifting superimposed by Luzon and Ryukyu subduction systems. J. Southeast Asian Earth Sci. 11, 73–80.

Chung, S.L., Lo, C.H., Lee, T.Y., Zhang, Y., Xie, Y., Li, X.H.,

Wang, K.L., Wang, P.L., 1998. Diachronous uplift of the Tibetan plateau starting 40 Myr ago. Nature 394, 769–773.

Chung, S.L., Wang, S.L., Shinjo, R., Lee, C.S., Chen, C.H., 2000. Initiation of arc magmatism in an embryo continental rifting zone of the southernmost part of Okinawa Trough. Terra Nova 12, 225–230.

Crawford, A.J., 1980. A clinoenstatite-bearing cumulate olivine pyroxenite from Howqua, Victoria. Contrib. Mineral. Petrol. 75, 353–367.

Dick, H.J.B., Bullen, T., 1984. Chromian spinel as a petrogenetic indicator in abyssal and alpine-type peridotites and spatially associated lavas. Contrib. Mineral. Petrol. 86, 54–76.

Edwards, C.M., Menzies, M.A., Thirlwall, M.F., Morris, J.D., Leeman, W.P., Harmon, R.S., 1994. The transition to potassic alkaline volcanism in island arcs: the Ringgit–Beser complex, east Java, Indonesia. J. Petrol. 35, 1557–1595.

Eggins, S.M., 1993. Origin and differentiation of picritic arc magmas, Ambae (Aoba), Vanuatu. Contrib. Mineral. Petrol. 114, 79–100.

Elliott, T., Plank, T., Zindler, A., White, W., Bourdon, B., 1997. Element transport from slab to volcanic front at the Mariana arc. J. Geophys. Res. 102, 14991–15019.

Falloon, T.J., Green, D.H., Hatton, C.J., Harris, K.L., 1988. Anhydrous partial melting of a fertile and depleted peridotie from 2 to 30 kb and application to basalt petrogenesis. J. Petrol. 29, 1257–1282.

Foley, S.F., 1992a. Petrological characterization of the source components of potassic magmas: geochemical and experimental constraints. Lithos 28, 187–204.

Foley, S.F., 1992b. Vein-plus-wall-rock melting mechanisms in the lithosphere and the origin of potassic alkaline magmas. Lithos 28, 435–453.

Foley, S.F., Venturelli, G., Green, D.H., Toscani, L., 1987. The ultrapotassic rocks: characteristics, classification, and constraints for petrogenetic models. Earth-Sci. Rev. 24, 81–134.

Gill, J.B., 1981. Orogenic Andesites and Plate Tectonics. Springer, Berlin, 390 pp.

Gill, J.B., Williams, R.W., 1990. Th isotope and U-series studies of subduction-related volcanic rocks. Geochim. Cosmochim. Acta 54, 1427–1442.

Goto, A., Tatsumi, Y., 1994. Quantitative analyses of rock samples by an X-ray fluorescence spectrography (I). Rigaku J. 11, 40–59.

Govindaraju, K., 1994. 1994 compilation of working values and sample description for 383 geostandards. Geostand. Newsl. 18, 1–158.

Hart, S.R., Reid, M.R., 1991. Rb/Cs fractionation: a link between granulite metamorphism and the S-process. Geochim. Cosmochim. Acta 55, 2379–2383.

Hofmann, A.W., 1988. Chemical differentiation of the Earth: the relation between mantle, continental crust, and oceanic crust. Earth Planet. Sci. Lett. 90, 297–314.

Hofmann, A.W., Jochum, K.P., Seufert, M., White, W.M., 1986. Nb and Pb in oceanic basalts: new constraints on mantle evolution. Earth Planet. Sci. Lett. 79, 33–45.

Huang, C.S., Chen, J.C., 1985. Geochemistry of absarokites from Tsaolingshan, northern Taiwan. Proc. Geol. Soc. China 28, 55–69.

Ichimura, T., 1943. Alkali basalt from Tsaolingshan. Trans. Nat. Hist. Soc. Formosa 33, 178–183 (in Japanese).

Juang, W.S., 1993. Diversity and origin of Quaternary basaltic magma series in northern Taiwan. Bull. Natl. Mus. Nat. Sci. 4, 125–166.

Kamenetsky, V.S., Sobolev, A.V., Joron, J.-L., Semet, M.P., 1995. Petrology and geochemistry of Cretaceous ultramafic volcanics from East Kamchatka. J. Petrol. 36, 637–662.

Kamenetsky, V.S., Crawford, A.J., Meffre, S., 2001. Factors controlling chemistry of magmatic spinel: an empirical study of associated olivine, Cr-spinel and melt inclusions from primitive rocks. J. Petrol. 42, 655–671.

Keppler, H., 1996. Constraints from partitioning experiments on the compositions of subduction-zone fluids. Nature 380, 237–240.

Kersting, A.B., Arculus, R.J., 1995. Pb isotope composition of Klyuchevskoy volcano, Kamchatka and North Pacific sediments: implications for magma genesis and crustal recycling in the Kamchatkan arc. Earth Planet. Sci. Lett. 136, 133–148.

Lan, C.Y., Lee, T., Wang Lee, C.M., 1990. The Rb–Sr isotopic record in Taiwan gneisses and its tectonic implication. Tectonophysics 183, 129–143.

Lee, C.T., Wang, Y., 1988. Quaternary stress changes in northern Taiwan and their tectonic significance. Proc. Geol. Soc. China 31, 154–168.

Liu, Y., Liu, H., Li, X.H., 1996. Simultaneous and precise determination of 40 trace elements in rock samples. Geochimica 25, 552–558 (in Chinese).

Luhr, J.F., 1997. Extensional tectonics and the diverse primitive volcanic rocks in the western Mexican volcanic belt. Can. Mineral. 35, 473–500.

Maury, R.C., Defant, M.J., Joron, J.-L., 1992. Metasomatism of the sub-arc mantle inferred from trace elements in Philippine xenoliths. Nature 360, 661–663.

McDonough, W.F., Sun, S.-S., 1995. Composition of the Earth. Chem. Geol. 120, 223–253.

McDonough, W.F., Sun, S.-S., Ringwood, A.E., Jagoutz, E., Hofmann, A.W., 1992. Potassium, rubidium, and cesium in the Earth and Moon and the evolution of the mantle of the Earth. Geochim. Cosmochim. Acta 56, 1001–1012.

Miller, D.M., Goldstein, S.L., Langmuir, C.H., 1994. Cerium/lead and lead isotope ratios in arc magmas and the enrichment of lead in the continents. Nature 368, 514–520.

Miller, C., Schuster, R., Klotzli, U., Frank, W., Purtsgheller, F., 1999. Post-collisional potassic and ultrapotassic magmatism in SW Tibet: geochemical and Sr–Nd–Pb–O isotopic constraints for mantle source characteristics and petrogenesis. J. Petrol. 40, 1399–1424.

Müller, D., Rock, N.M.S., Groves, D.I., 1992. Geochemical discrimination between shoshonitic and potassic volcanic rocks in different tectonic settings: a pilot study. Mineral. Petrol. 46, 259–289.

Pearce, J.A., Baker, P.E., Harvey, P.K., Luff, I.W., 1995. Geochemical evidence for subduction fluxes, mantle melting and fractional crystallization beneath the South Sandwich island arc. J. Petrol. 36, 1073–1109.

Peccerillo, A., 1999. Multiple mantle metasomatism in central–southern Italy: geochemical effects, timing and geodynamic implications. Geology 27, 315–318.

Peccerillo, A., Taylor, D.R., 1976. Geochemistry of Eocene calc-alkaline volcanic rocks from Kastamonu area, Northern Turkey. Contrib. Mineral. Petrol. 58, 63–91.

Robert, U., Foden, J., Varne, R., 1992. The Dodecanese Province, SE Aegean: a model for tectonic control on potassic magmatism. Lithos 28, 241–260.

Rogers, N.W., Hawkesworth, C.J., Mattey, D.P., Harmon, R.S., 1987. Sediment subduction and the source of potassium in orogenic leucitites. Geology 15, 451–453.

Rudnick, R.L., Fountain, D.M., 1995. Nature and composition of the continental crust: a lower crustal perspective. Rev. Geophys. 33, 267–309.

Ryerson, F.J., Watson, E.B., 1987. Rutile saturation in magmas: Implications for Ti–Nb–Ta depletion in island-arc basalts. Earth Planet. Sci. Lett. 86, 225–239.

Schaefer, B.F., Turner, S.P., Rogers, N.W., Hawkesworth, C.J., Williams, H.M., Pearson, D.G., Nowell, G.M., 2000. Re–Os isotope characteristics of postorogenic lavas: implications for the nature of young lithospheric mantle and its contribution to basaltic magmas. Geology 28, 563–566.

Schmidt, K.H., Bottazzi, P., Vannucci, R., Mengel, K., 1999. Trace element partitioning between phlogopite, clinopyroxene and leucite lamproite melt. Earth Planet. Sci. Lett. 168, 287–299.

Shinjo, R., Chung, S.L., Kato, Y., Kimura, M., 1999. Geochemical and Sr-Nd isotopic characteristics of volcanic rocks from the Okinawa Trough and Ryukyu Arc: implications for the evolution of a young, intracontinental back arc basin. J. Geophys. Res. 104, 10591–10608.

Sibuet, J.-C., Hsu, S.K., Shyu, C.T., Liu, C.S., 1995. Structural and kinematic evolutions of the Okinawa Trough backarc basin. In: Taylor, B. (Ed.), Backarc Basins: Tectonics and Magmatism. Plenum, New York, pp. 343–379.

Sigurdsson, I.A., Kamenetsky, V.S., Crawford, A.J., Eggins, S.M., Zlobin, S.K., 1993. Primitive island arc and oceanic lavas from the Hunter Ridge-Hunter fracture zone: evidence from glass, olivine and spinel compositions. Mineral. Petrol. 47, 149–169.

Sun, S.-S., 1980. Lead isotopic study of young volcanic rocks from mid-ocean ridges, ocean islands and island arcs. Philos. Trans. R. Soc. London, Ser. A 297, 409–445.

Sun, S.-S., McDonough, W.F., 1989. Chemical and isotopic systematics of oceanic basalts: implications for mantle composition and processes. In: Saunders, A.D., Norry, M.J. (Eds.), Magmatism in the Ocean Basins. Geol. Soc. Spec. Publ., vol. 42, pp. 313–345.

Suppe, J., 1981. Mechanics of mountain building in Taiwan. Mem. Geol. Soc. China 4, 67–89.

Tatsumi, Y., Kogiso, T., 1997. Trace element transport during dehydration processes in the subducted oceanic crust: 2. Origin of chemical and physical characteristics in arc magmatism. Earth Planet. Sci. Lett. 148, 207–221.

Tatsumi, Y., Hamilton, D.L., Nesbitt, R.W., 1986. Chemical characteristics of fluid phase released from a subducted lithosphere and origin of arc magmas: evidence from high-pressure experiments and natural rocks. J. Volcanol. Geotherm. Res. 29, 293–309.

Taylor, S.R., McLennan, S.M., 1985. The Continental Crust: Its Composition and Evolution. Blackwell, Cambridge, 312 pp.

Teng, L.S., 1990. Geotectonic evolution of late Cenozoic arc–continent collision in Taiwan. Tectonophysics 183, 57–76.

Teng, L.S., 1996. Extensional collapse of the northern Taiwan mountain belt. Geology 24, 949–952.

Tsai, Y.B., 1986. Seismotectonics of Taiwan. Tectonophysics 125, 17–38.

Turner, S.P., Platt, J.P., George, R.M.M., Kelley, S.P., Pearson, D.G., Nowell, G.M., 1999. Magmatism associated with orogenic collapse of the Betic–Alboran domain, SE Spain. J. Petrol. 40, 1011–1036.

Varne, R., 1985. Ancient subcontinental mantle: a source for K-rich orogenic volcanics. Geology 13, 405–408.

Walker, D.A., Cameron, W.E., 1983. Boninite primary magmas: evidence from Cape Vogel Peninsula, PNG. Contrib. Mineral. Petrol. 83, 150–158.

Wang, K.L., 2000. Geochemistry and petrogenesis of the late Pliocene–Quaternary volcanic rocks from the Northern Taiwan Volcanic Zone. Unpubl. PhD thesis, Nat'l Taiwan Univ., Taipei, 169 pp. (in Chinese).

Wang, K.L., Chung, S.L., Chen, C.H., Shinjo, R., Yang, T.F., Chen, C.-H., 1999. Post-collisional magmatism around northern Taiwan and its relation with opening of the Okinawa Trough. Tectonophysics 308, 363–376.

Yang, H.J., Chen, J.C., Yang, H.Y., 1987. Geochemistry of ultramafic nodules in basaltic rocks from Peiliao, Penghu Islands and Liutsu, northern Taiwan. Proc. Geol. Soc. China 30, 44–57.

Yeh, Y.H., Barrier, E., Lin, C.H., Angelier, J., 1991. Stress tensor analysis in the Taiwan area from focal mechanisms of earthquakes. Tectonophysics 200, 267–280.

Yen, T.P., 1949. A priliminary study on the alkaline basalt of Tsaolingshan, Taiwan. Bull. Geol. Surv. Taiwan 2, 1–23.

You, C.F., Castillo, P.R., Gieskes, J.M., Chan, L.H., Spivack, A.J., 1996. Trace element behavior in hydrothermal experiments: implications for fluid phases at shallow depths in subduction zones. Earth Planet. Sci. Lett. 140, 41–52.

Yu, S.B., Chen, H.Y., 1994. Global positioning system measurements of crustal deformation in the Taiwan arc-continent collision zone. Terr. Atmos. Ocean Sci. 5, 477–498.

Zhang, M., Sudabby, P., Thompson, R.N., Thirlwall, M.F., Menzies, M.A., 1995. Potassic volcanic rocks in NE China: geochemical constraints on mantle source and magma genesis. J. Petrol. 36, 1275–1303.